AD-A054 806 SRI INTERNATIONAL MENLO PARK CA F/G 20/5
LIDAR OBSERVATIONS OF SMOKE AND DUST CLOUDS AT 0.7-MICROMETER A--ETC(U)
APR 78 E E UTHE DAAG29-77-C-0001
UNCLASSIFIED ARO-13833.2-GS NL

1 OF 1
AD
A054 806

END
DATE FILMED
7-78
DDC

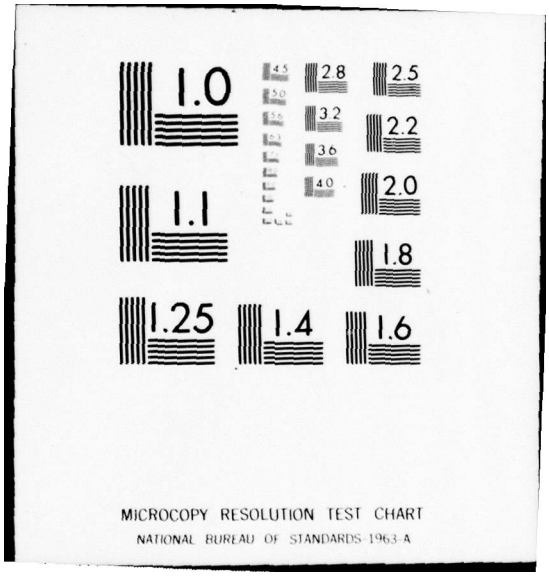
1.0
1.1
1.25
1.4
1.6
1.8
2.0
2.2
2.5
2.8
3.2
3.6
4.0
4.5
5.0
MICROCOPY RESOLUTION TEST CHART
NATIONAL BUREAU OF STANDARDS-1963-A

ARO 13833.2-GS

8

Technical Report 1

LIDAR OBSERVATIONS OF SMOKE AND DUST CLOUDS AT 0.7-μm AND 10.6-μm WAVELENGTHS

By: E. E. UTHE

Prepared for:

U.S. ARMY RESEARCH OFFICE
GEOSCIENCES DIVISION
RESEARCH TRIANGLE PARK
NORTH CAROLINA 27709

and

ATMOSPHERIC SCIENCES LABORATORY
WHITE SANDS MISSILE RANGE
NEW MEXICO 88002

ARO CONTRACT DAAG29-77-C-0001

333 Ravenswood Avenue
Menlo Park, California 94025 U.S.A.
(415) 326-6200
Cable: STANRES, Menlo Park
TWX: 910-373-1246

SRI International

SRI International

Technical Report 1 *April 1978*

LIDAR OBSERVATIONS OF SMOKE AND DUST CLOUDS AT 0.7-μm AND 10.6-μm WAVELENGTHS

By: E. E. UTHE

Prepared for:

U.S. ARMY RESEARCH OFFICE
GEOSCIENCES DIVISION
RESEARCH TRIANGLE PARK
NORTH CAROLINA 27709

and

ATMOSPHERIC SCIENCES LABORATORY
WHITE SANDS MISSILE RANGE
NEW MEXICO 88002

ARO CONTRACT DAAG29-77-C-0001

SRI Project 5862

Approved by:

R.T.H. COLLIS, *Director*
Atmospheric Sciences Laboratory

Copy No. 10

333 Ravenswood Avenue • Menlo Park, California 94025 • U.S.A.

SRI International

SECURITY CLASSIFICATION OF THIS PAGE (When Data Entered)

REPORT DOCUMENTATION PAGE

READ INSTRUCTIONS BEFORE COMPLETING FORM

1. REPORT NUMBER: ARO 13833.2-GS
2. GOVT ACCESSION NO.
3. RECIPIENT'S CATALOG NUMBER

4. TITLE (and Subtitle): LIDAR OBSERVATIONS OF SMOKE AND DUST CLOUDS AT 0.7-μm AND 10.6-μm WAVELENGTHS. micrometers

5. TYPE OF REPORT & PERIOD COVERED: Technical Report No. 1, Covering the Period January 1977 to April 1978

6. PERFORMING ORG. REPORT NUMBER: SRI Project 5862

7. AUTHOR(s): Edward E. Uthe

8. CONTRACT OR GRANT NUMBER(s): Contract DAAG29-77-C-0001

9. PERFORMING ORGANIZATION NAME AND ADDRESS:
SRI International
333 Ravenswood Avenue
Menlo Park, California 94025

10. PROGRAM ELEMENT, PROJECT, TASK AREA & WORK UNIT NUMBERS

11. CONTROLLING OFFICE NAME AND ADDRESS:
U.S. Army Research Office
Geosciences Division
Research Triangle Park, North Carolina 27709

12. REPORT DATE: April 1978
13. NO. OF PAGES: 32

14. MONITORING AGENCY NAME & ADDRESS (if diff. from Controlling Office): SRI-TR-1. 33 pp.

15. SECURITY CLASS. (of this report): UNCLASSIFIED

15a. DECLASSIFICATION/DOWNGRADING SCHEDULE

16. DISTRIBUTION STATEMENT (of this report)

Approved for public release; distribution unlimited.

DDC RELEASED JUN 7 1978

17. DISTRIBUTION STATEMENT (of the abstract entered in Block 20, if different from report)

18. SUPPLEMENTARY NOTES

The findings in this report are not to be construed as an official Department of the Army position, unless so designated by other authorized documents.

19. KEY WORDS (Continue on reverse side if necessary and identify by block number)

Dense smoke
Military smoke
Lidar
Optical properties
Backscatter
Transmission
Multi-wavelength
microwaves

20. ABSTRACT (Continue on reverse side if necessary and identify by block number)

An experimental program was conducted for the purpose of deriving basic data required to determine the capabilities of 10.6-μm-wavelength lidar systems for observation of dense smoke aerosols and for determining specifications for procuring an optimum lidar system for this application.

A 10.6-μm-wavelength CO_2 mobile lidar system was constructed and interfaced to the data-processing electronics of the 0.7-μm-wavelength Mark IX mobile lidar system. The real-time minicomputer-based data system of the

→ next Page

DD FORM 1 JAN 73 1473
EDITION OF 1 NOV 65 IS OBSOLETE

SECURITY CLASSIFICATION OF THIS PAGE (When Data Entered)

19. KEY WORDS (Continued)

20 ABSTRACT (Continued)

Mark IX lidar was programmed for intensity-modulated TV pictorial display of backscatter data collected from the two lidar systems on an alternate-firing basis. The two-lidar system was transported to Dugway Proving Ground and participated in scheduled tests involving the generation of dense smoke aerosols.

Data collected on smoke aerosols and also on road dust consisting of larger-sized particles show that while the 10.6-μm system is slightly more sensitive to road dust, it is very insensitive to smoke, and only very dense smokes can be observed. The data illustrate that aerosol type strongly affects the wavelength dependence of backscatter and attenuation. These experimental results are consistent with theoretical data. Theoretical results also indicate that a 3-to-4-μm-wavelength lidar would provide the best measure of aerosol physical density independent of uncertainties in particle size.

Because (1) more accurate inferences of aerosol densities might result, (2) short-wavelength (0.7 μm) systems cannot penetrate dense smoke aerosols, and (3) long-wavelength (10.6 μm) systems are insensitive to smoke aerosols, it is suggested that a 3-to-4-μm-wavelength lidar may be the optimum system for this application.

CONTENTS

ILLUSTRATIONS

TABLE

ACKNOWLEDGMENTS

The author is indebted to Dr. Edward R. Murray and Mr. Jan E. van der Laan for design and construction of the CO_2 lidar system. Jan van der Laan and Norman Nielsen operated the lidar systems at Dugway Proving Ground and Roy Endlich provided most of the computer data analysis. Ray Loveland of the Atmospheric Sciences Laboratory, White Sands Missile Range, provided very helpful suggestions both before and during the field program.

I INTRODUCTION

SRI International is conducting a three-year investigation funded by the Army Research Office, Division of Geophysics, to develop real-time digital lidar techniques for evaluation of aerosol, cloud, and precipitation optical and physical densities. During the initial phase of this study, several discussions were held with personnel of Army research centers, and several military-related conferences were attended, for the purpose of identifying current problem areas related to our study. By far, most interest was in a method to measure the three-dimensional distribution of density and optical parameters of dense smoke clouds. Based on previous experience with short- and long-wavelength lidar systems, SRI suggested an experiment to collect basic data on generated smoke clouds with a two-wavelength lidar (0.7 and 10.6 μm) built around the digital data processing and display capabilities of the SRI Mark IX mobile lidar system. Required additional funding was provided by the Atmospheric Sciences Laboratory, White Sands Missile Range, to construct a 10.6-μm mobile lidar component for the 0.7-μm Mark IX mobile system and to conduct a two-wavelength lidar field program to observe military smoke clouds generated at the Dugway Proving Ground. The major objective was to determine specifications for an optimum lidar system for observation of dense smoke. This report presents the results from this inital field effort.

II BACKGROUND

Lasers provide a source of light energy with the characteristics necessary for strong interaction with atmospherically suspended particulate matter at remote distances. Recognizing this soon after the development of the first laser, scientists at SRI began a series of experiments in 1963 to develop and apply single-ended, range-resolved lidar (laser-radar) techniques. A product of this development program is the SRI Mark IX mobile lidar system. Operated from a mobile platform (see Figure 1) provided with power-generating facilities, it can be transported to any location for immediate operation. The Mark IX specifications are listed in Figure 1.

One of the Mark IX's principal features is the use of a digital data recording, processing, and display system for real-time viewing of pictorial displays of atmospheric structure (Uthe and Allen, 1975). For example, Figure 2 presents a cross section of a smoke plume observed as the lidar was scanned in elevation at a constant azimuth directed perpendicular to the plume transport direction. Picture brightness is proportional to the logrithm of backscattered energy observed by the lidar receiver and can be related to plume density if attenuation of the laser energy by the plume particulates is ignored and if the backscatter-to-density ratio is constant for the region of plume observed. Vertical density profiles are plotted for the horizontal distances from the lidar indicated by the marks drawn above the plume. Techniques for quantitatively evaluating plume density (mass concentration) are further discussed by Johnson and Uthe (1971), and Uthe and Wilson (1977).

As the plume becomes more dense, backscatter returns from the far side of the plume may decrease because of increased attenuation of the laser energy by the intervening plume particulates. At longer wavelengths the attenuation normally is smaller; therefore, dense aerosol clouds may be better viewed with lidar systems operating at longer wavelengths than the 0.7-μm-wavelength Mark IX. However, at longer wavelengths the backscatter coefficient tends to decrease and detector sensitivity typically decreases also. The purpose of this study was to experimentally evaluate the use of a long-wavelength (10.6 μm) lidar system for remote observation of dense smoke aerosols and to derive specifications for an optimum lidar system for this purpose.

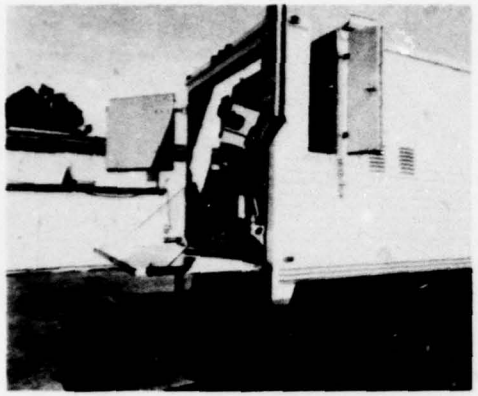

(a) MARK IX LIDAR VAN

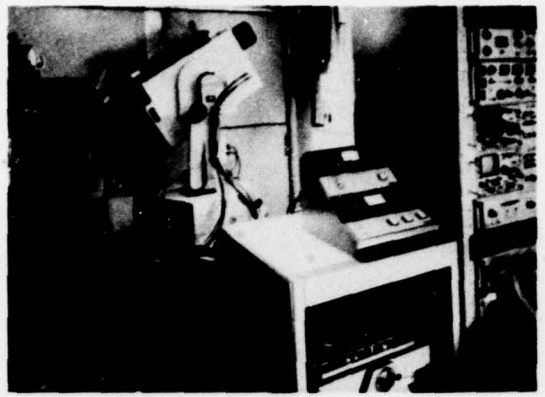

(b) ANALOG DATA AND FIRE CONTROL ELECTRONICS

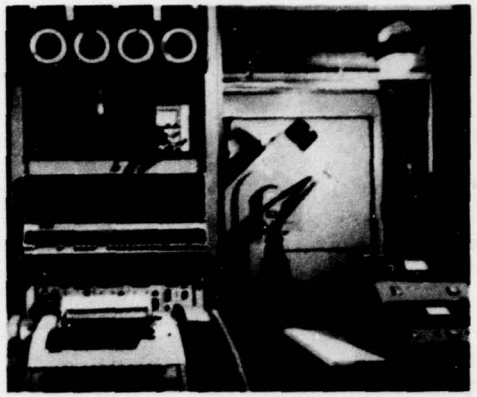

(c) DIGITAL DATA ELECTRONICS AND TV DISPLAY

EXTERIOR AND INTERIOR VIEWS OF THE LIDAR VAN

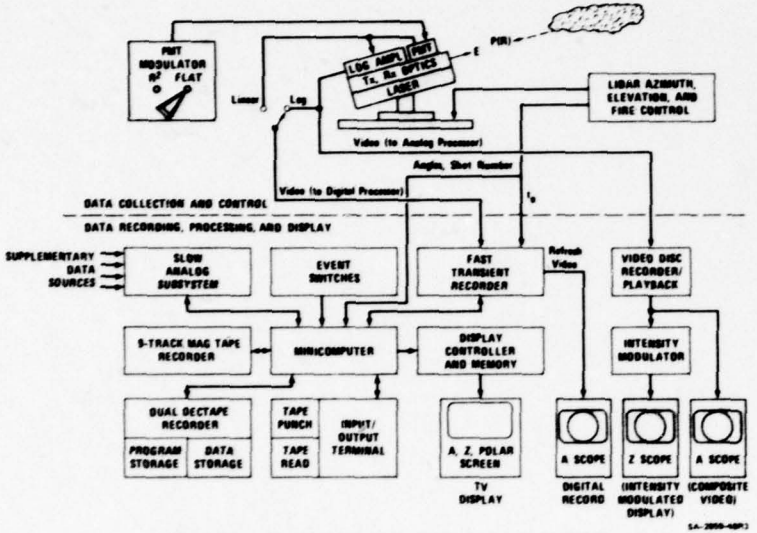

BLOCK DIAGRAM OF THE LIDAR SYSTEM

LIDAR SPECIFICATIONS

TRANSMITTER

6943A Wavelength
0.5 mrad Beamwidth
1.0 J Pulse Energy
30 ns Pulse Length
60 ppm Maximum PRF

RECEIVER

6 inch Newtonian
1 to 5 mrad Field of View
5A Predetection Filter
RCA 7265 PMT Detector
4-decade, 35-MHz Logarithmic Amplifier, Inverse-range-squared or step-function PMT modulation.

DATA SYSTEMS

Analog video disc recording (4.5 MHz) with A-scope and Z-scope real-time displays. Digital magnetic tape (data and programs) recording (25 MHz) with computer processing and real-time TV display (512 x 256 x 4 bit) of processed data.

MOUNT

Automatic azimuth and elevation fire and scan with 0.1° minimum resolution. Automatic reset. Mechanical safety stops.

TA-653583-311

FIGURE 1 THE SRI MARK IX MOBILE LIDAR SYSTEM

III EXPERIMENTAL PROGRAM

A. *Equipment*

At the start of this program, a laboratory CO_2 lidar system was already being operated at SRI as part of an ongoing effort to develop instrumentation for range-resolved measurements of gas concentrations using well-known two-wavelength differential absorption of scattered energy (DASE) and differential absorption lidar (DIAL) techniques. Clear-air aerosol distributions could be observed over path lengths up to 4 km. Therefore, a system of similar design would provide adequate sensitivity for observation over a 1-km path to be used in this study. However, unlike the laboratory model, the field lidar components were to be operated together within a van that would be located next to the Mark IX lidar van. Therefore, radio frequencies (emitted by the CO_2 laser) and other interference problems could develop. Special shielding for the infrared detector assembly was constructed and the number of interconnecting cables to the Mark IX lidar van was kept to a minimum.

A picture of the CO_2 lidar is presented in Figure 3, a block diagram of the two lidar system is shown in Figure 4, and specifications of the two systems are given in Table 1. The fire rate is determined from the CO_2 lidar van. Basically, the CO_2 system is given a "fire" command, and this is input to the ruby lidar fire-control electronics. The CO_2 laser is pulsed and backscattered energy is collected by a 12-inch-diameter telescope and routed to a liquid-nitrogen-cooled HgCdTe detector. After amplification, the signal is input to the Mark IX logarithmic amplifier and is digitized, recorded, and processed for display by a minicomputer-based data system. About 1 s after the CO_2 laser is pulsed, the ruby laser is fired and backscattered energy is collected by a 6-inch-diameter telescope and routed to a photomultiplier detector after passing through a narrowband interference filter to reduce effects of background light levels. The signal is then processed by the same electronics used for the CO_2 lidar backscatter signature. The output of an integrating nephelometer that measures in-situ aerosol scattering coefficient is sampled at the time of the ruby laser firing, and this value is also input to the minicomputer for recording and analysis. A computer program was written for real-time TV display of CO_2 and ruby backscatter signatures as an intensity-modulated split-screen picture that also included a plot of the nephelometer output. The system was checked out at SRI in Menlo Park, California, and was then transported to Dugway Proving Ground, Utah, to participate in a scheduled dense smoke observational program.

B. *Field Configuration*

The CO_2 and ruby (Mark IX) lidar vans were positioned near the instrumentation buildings of the horizontal grid at Dugway Proving Ground. The lidar systems were operated from line power rather than from the van-mounted generators. A red colored target was placed at the far end of the grid so that the lidar-to-target path was parallel to the grid of aerosol samplers operated by Dugway. The target stopped laser energy and prevented it from being an eye hazard beyond the target, and provided a constant reflective surface so that lidar-observed

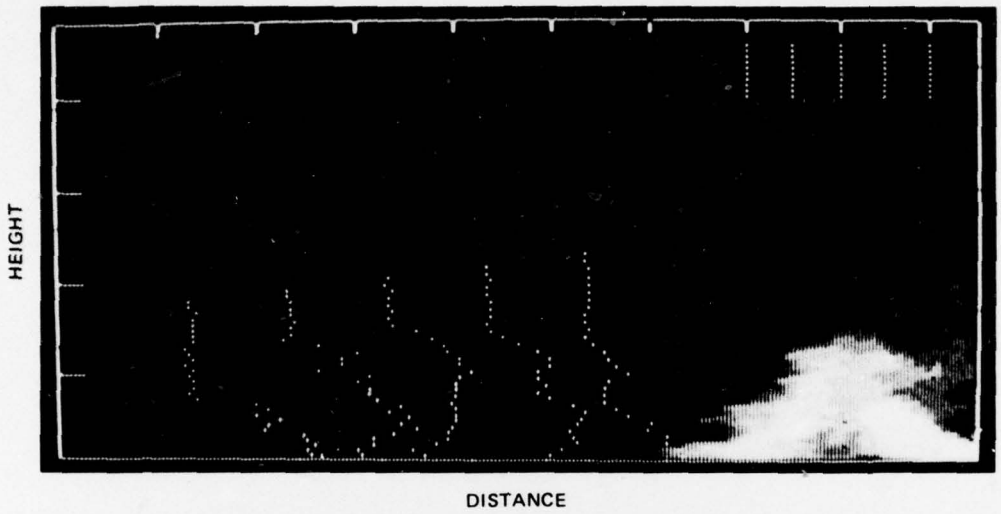

FIGURE 2 EXAMPLE OF COMPUTER-GENERATED VERTICAL PLUME DENSITY PROFILES. Lidar is located at lower left corner. The height and distance scale is 75 m/div. Plume vertical concentrations (relative to clear air with a scale of 10 dB/div) are plotted at the lower left and the horizontal position associated with each profile is plotted in the upper right.

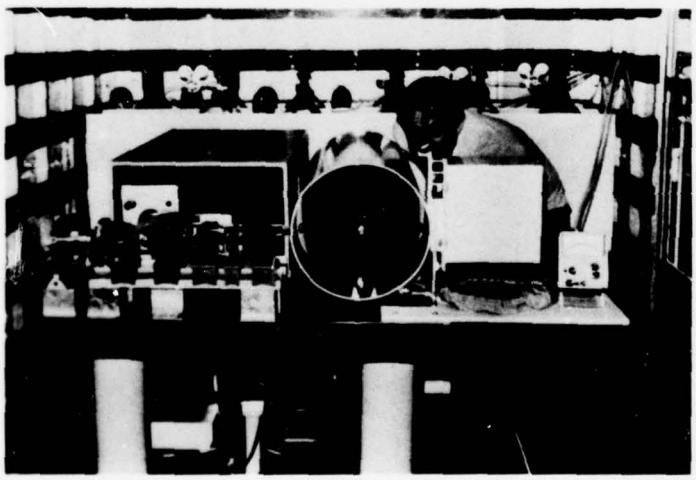

FIGURE 3 CO_2 LIDAR SYSTEM

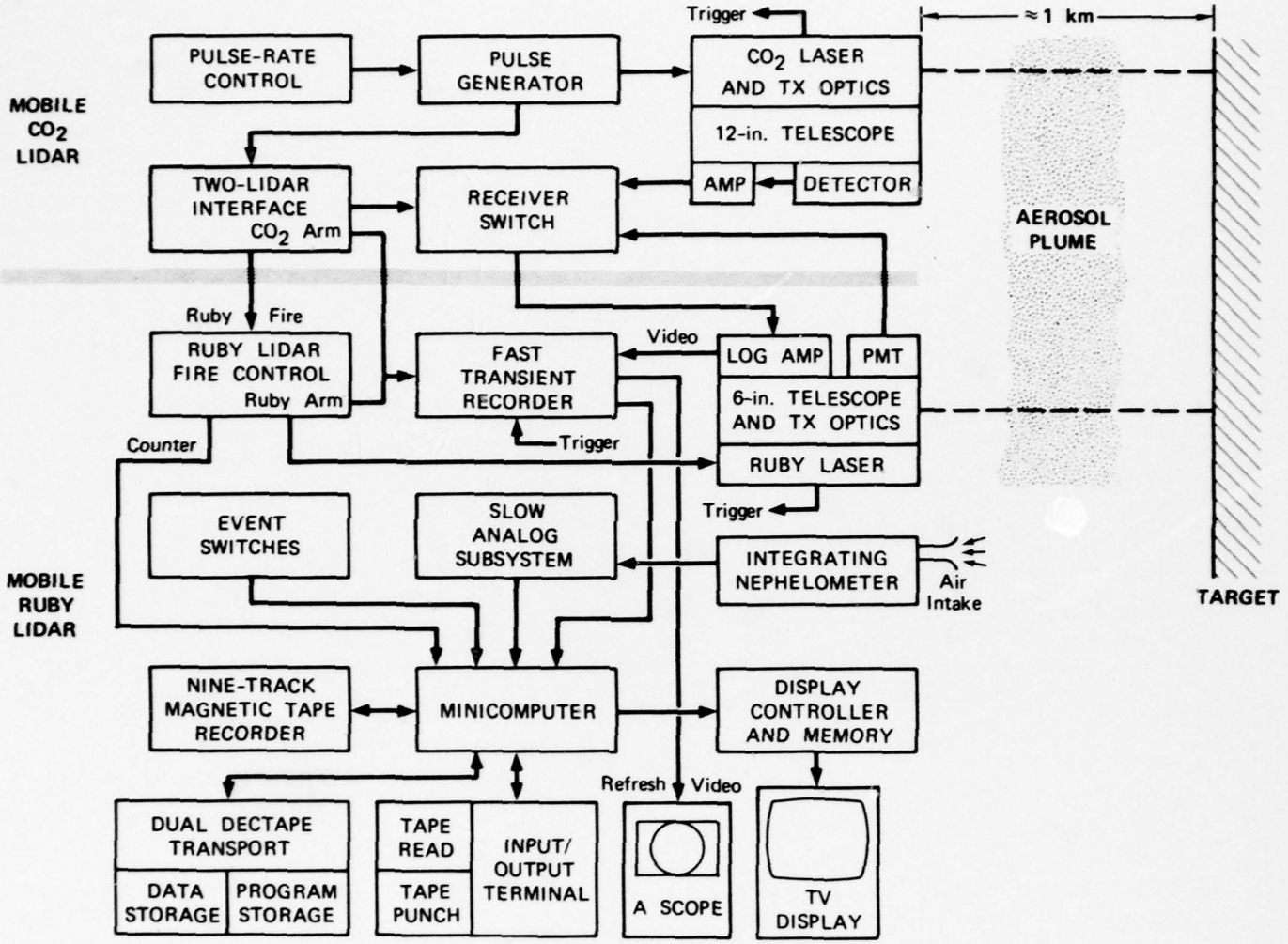

FIGURE 4 BLOCK DIAGRAM OF THE TWO-WAVELENGTH (0.7 and 10.6 μm) LIDAR SYSTEM

Table 1

CO_2 AND RUBY LIDAR SPECIFICATIONS

	CO_2 Lidar	Ruby Lidar
Transmitter		
Manufacturer	Lumonics Research, Inc.	Holobeam
Model	TEA-101-2	300
Type	CO_2	Ruby
Wavelength	10600 nm	694 nm
Beam Diameter	3.1 cm	2 cm
Beam Divergence	1.2 mrad	0.5 mrad
Operation	Pulsed	Q-switched
Energy	≈1 J	≈1 J
PRF (maximum)	1 pps	1 pps
Pulsewidth	100 ns	30 ns
Receiver		
Telescope	12-inch Newtonian	6-inch Newtonian
Detector	Infrared Associates, HgCdTe-cooled. Detectivity 1.1×10^{10} cm Hz/watt.	RCA 7265 PMT
Predetection Filter	None	5 Å

reflected energy can be used to monitor atmospheric transmission over the lidar-to-target path. The CO_2 lidar-to-target path was measured as 1014.4 m long, and the ruby lidar-to-target path was measured as 1006.1 m. Figure 5 is a drawing of the experimental configuration. A dirt road ran parallel to the grid, and road dust could be generated by driving a car along the road. The road dust consists of much larger particle sizes than generated smokes; therefore the wavelength dependence of backscatter and attenuation on particle size could be easily investigated. Results obtained from scheduled smoke generating tests conducted by Dugway and a special road dust/smoke test conducted by SRI are presented in the next section of this report.

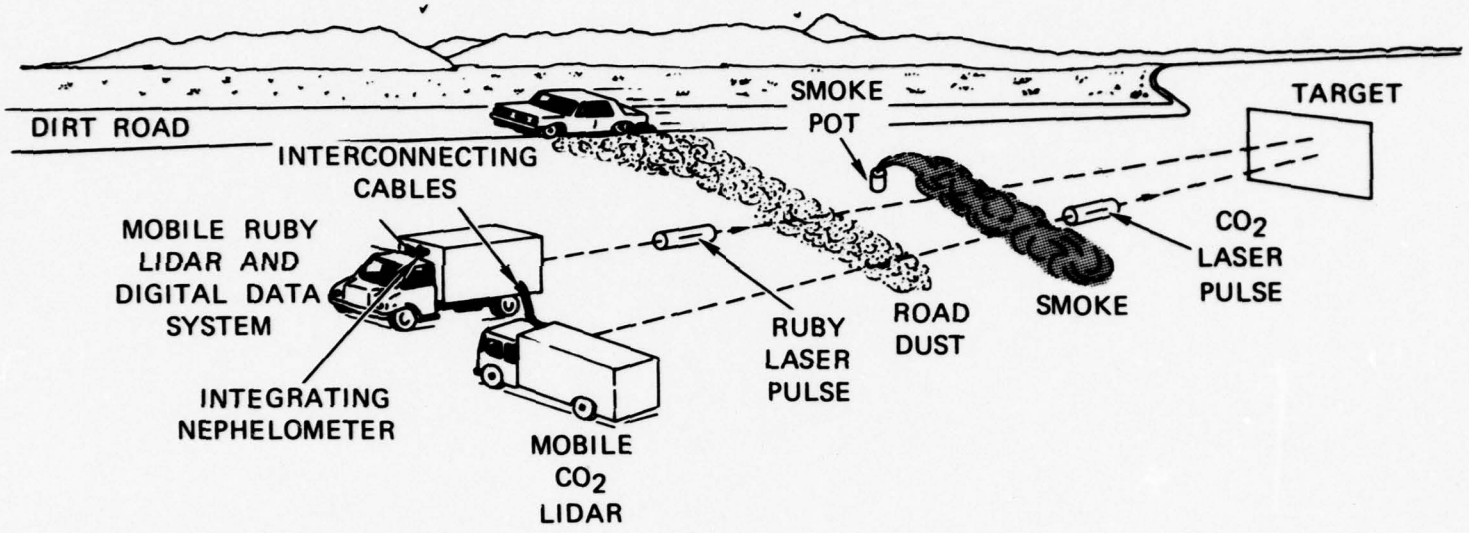

FIGURE 5 DRAWING OF THE EXPERIMENTAL CONFIGURATION FOR THE TWO-WAVELENGTH LIDAR OBSERVATION OF SMOKE AND ROAD DUST

IV RESULTS OF LIDAR OBSERVATIONS

A. *Calibration of the Lidar Response*

The response of the Mark IX lidar receiver to laser energy backscattered by the atmosphere is normally well characterized by applying standard calibration techniques several times a year. However, the Dugway experiments involved the use of a new lidar component (the 10.6-μm system) interfaced with the Mark IX electronics, and this may have had an effect on their response characteristics. Moreover, the relatively large energy reflected from the target located only 1-km from the lidar might have saturated the detector or receiver electronics so that normal lidar response characteristics would no longer be valid. Because of limited operational time at Dugway, a complete calibration run was not attempted. However, a limited calibration run was conducted to provide data to investigate lidar response characteristics. The method and results of this calibration are discussed below.

The Mark IX detector response can be adjusted by two variable range gates, with each gate containing an electrical attenuator that can be stepped in 10-dB (one order of magnitude response to light intensity) increments. For all the Dugway tests (including the calibration run), the first range gate was adjusted to turn off just before the range of the target return, and the second range gate turned on at this point. Therefore, the Mark IX detector sensitivity for the backscatter along the lidar-to-target path and for the target return could be adjusted independently.

The calibration run consisted of firing both lidar systems while incrementing the gate attenuation values on the 0.7-μm lidar system and placing optical attenuators in the path of the 10.6-μm lidar system. The results of this calibration is shown in Figure 6. The backscatter data have been linearized using the Mark IX calibration value that relates receiver light input to digitizer output (0.2 dB/count). Atmospheric backscatter observed with the 0.7-μm lidar and target returns observed with the 10.6-μm lidar behaved as expected (one-order-of-magnitude signal decrease for each 10-dB filter). However, the target returns observed with the 0.7-μm lidar show that the large light levels saturated the receiver/detector system, and the lidar response was nonlinear. Nevertheless, the data were used to derive a lidar response function (Figure 7) for correcting for the nonlinearity in computations of atmospheric transmission based on target returns.

B. *Road Dust and Smoke Comparison Tests*

On 19 September 1977, before the scheduled smoke tests, SRI conducted a special test designed to determine the effect of particle size on the wavelength dependence of backscatter and transmission. Red and white smoke grenades and a moving automobile were used to generate smoke and road dust (see Figure 5). The smoke consisted mostly of near-micron-diameter particles, while the road dust mostly consisted of larger particles. (However, a detailed size analysis was not conducted by SRI.) An intensity-modulated pictorial display generated from recorded backscatter signatures is shown in Figure 8. Brightness of the display is pro-

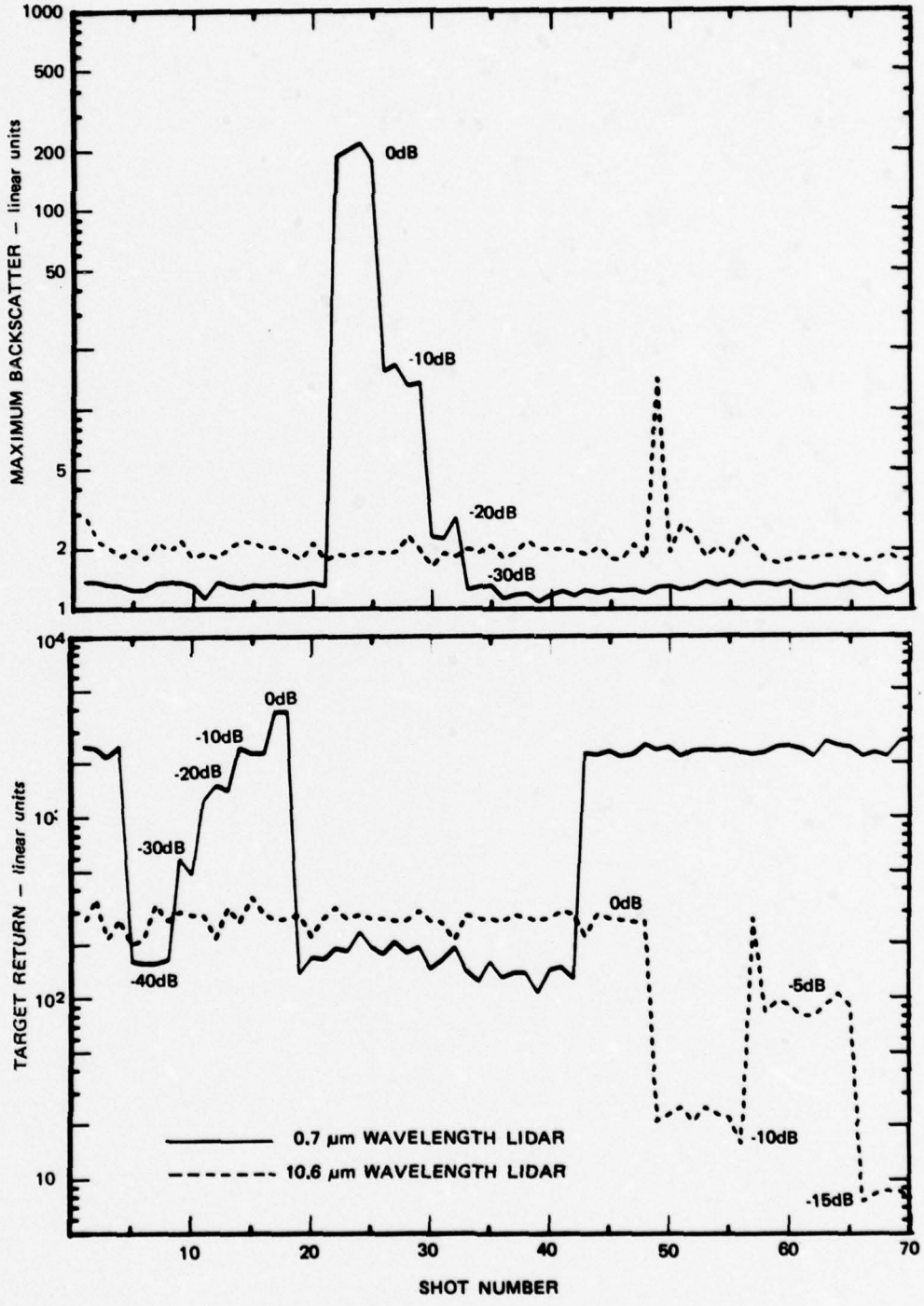

FIGURE 6 DUGWAY LIDAR CALIBRATION

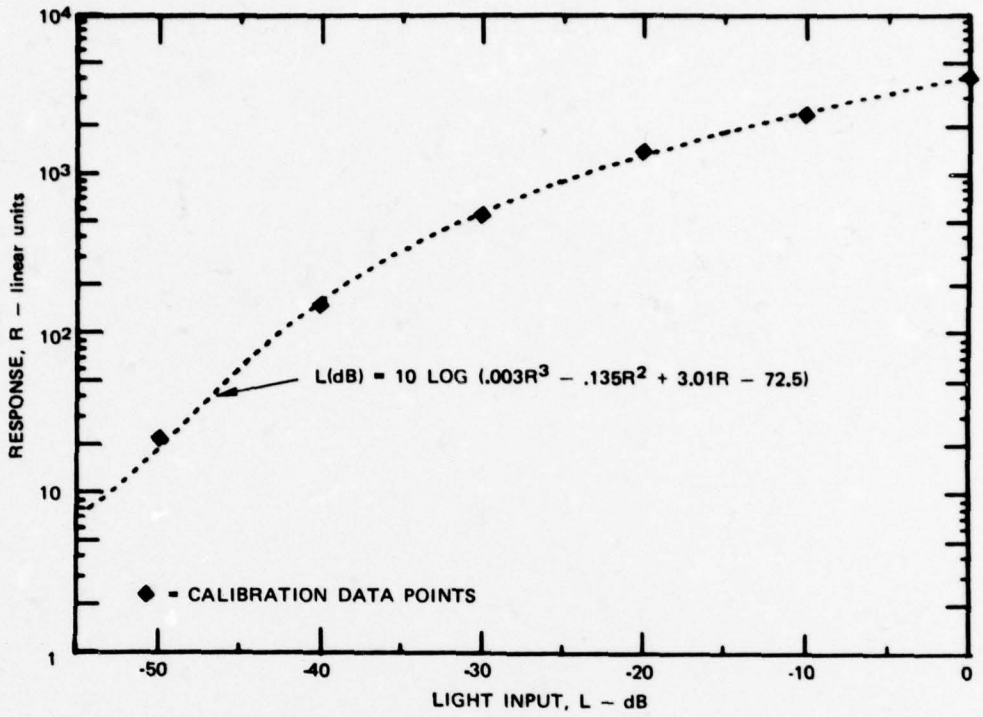

FIGURE 7 LIDAR RESPONSE FUNCTION USED TO CORRECT FOR NONLINEAR TARGET RETURNS

portional to the logrithm of the light intensity observed by the lidar receivers. The inverted V patterns are caused by backscattering from aerosols generated by the automobile moving from the lidar site to the target and then returning to the lidar site. These patterns are observed by both the 0.7- and 10.6-μm wavelength lidar systems. Other data presented later in this report show that the 10.6-μm wavelength lidar system was a more sensitive detector of the large-particle-size dust than was the 0.7-μm wavelength system. However, as shown in Figure 8, the long-wavelength system did not detect the red or white smoke that is readily observed on the backscatter records of the short-wavelength lidar.

Figures 9 and 10 present data plots of atmospheric transmission over the lidar/target path and the maximum backscatter observed over the path for both the 0.7-and 10.6-μm wavelength lidar systems during time periods of smoke and dust generation. The transmission data are based on the target returns and are normalized to 100% for the maximum observed return over the time period analyzed. The backscatter data have been normalized to 1.0 for the minimum observed value and therefore represent a backscatter ratio of smoke and clear air to clear air.

The data presented in Figure 9 were collected with a less sensitive CO_2 lidar receiver (-10dB) in order to reduce return signals to within saturation limits of the analog processing electronics. Even with reduced sensitivity, backscatter from the dust is more than 10 dB above background returns observed during clear air conditions. The transmission as a function of time is very similar for both wavelengths, indicating large particle sizes. However, for red

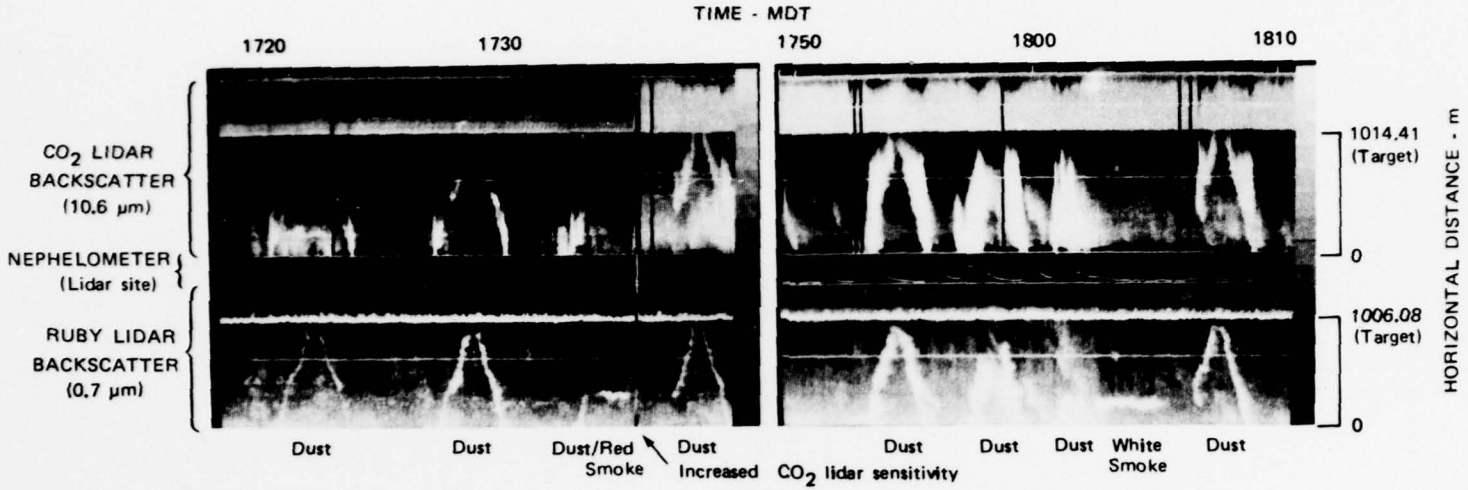

FIGURE 8 INTENSITY-MODULATED TV DISPLAY OF CO_2 AND RUBY LIDAR OBSERVATION OF ROAD DUST (generated by driving car along road) AND RED AND WHITE SMOKE

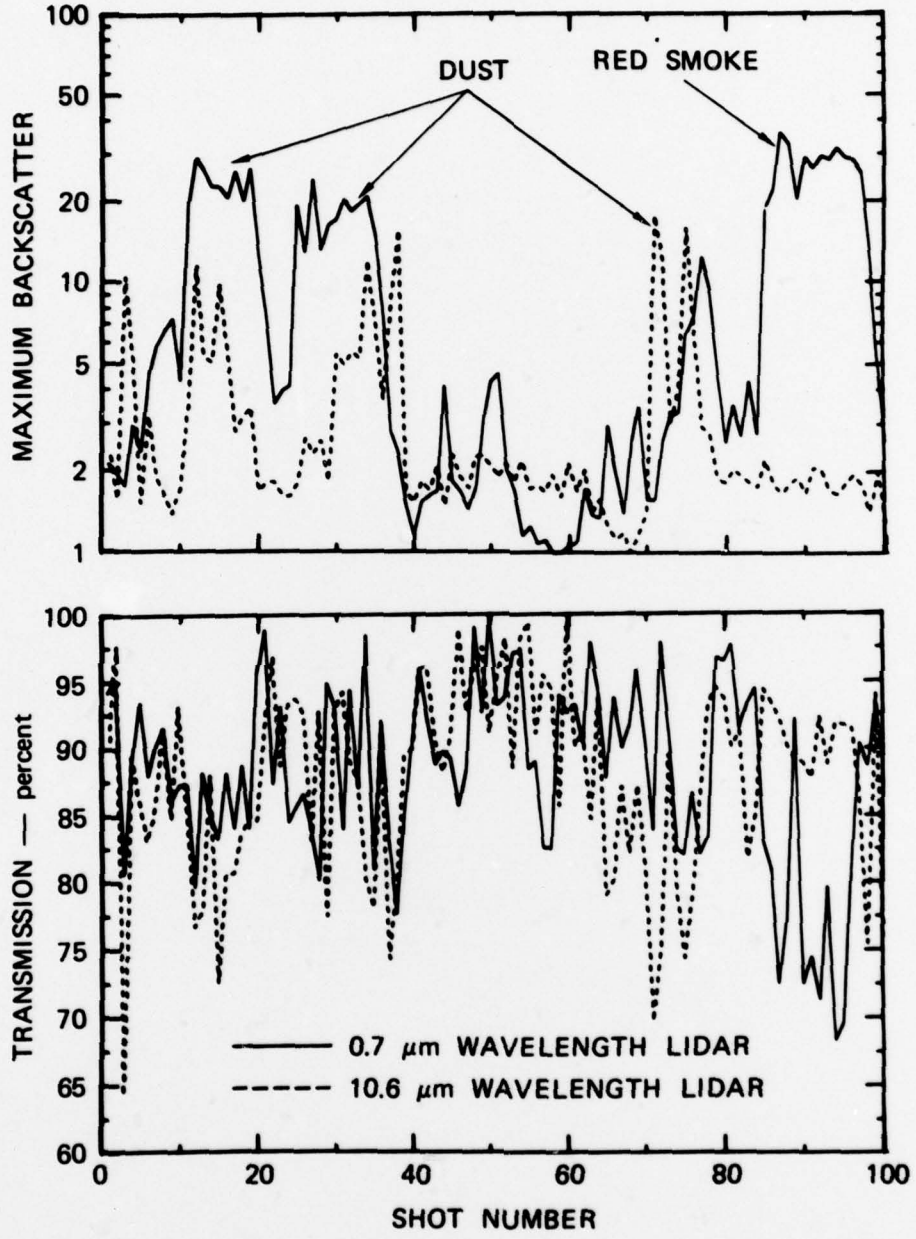

FIGURE 9 TRANSMISSION AND MAXIMUM BACKSCATTER OBSERVED BY THE TWO-WAVELENGTH LIDAR SYSTEM FOR ROAD DUST AND RED SMOKE

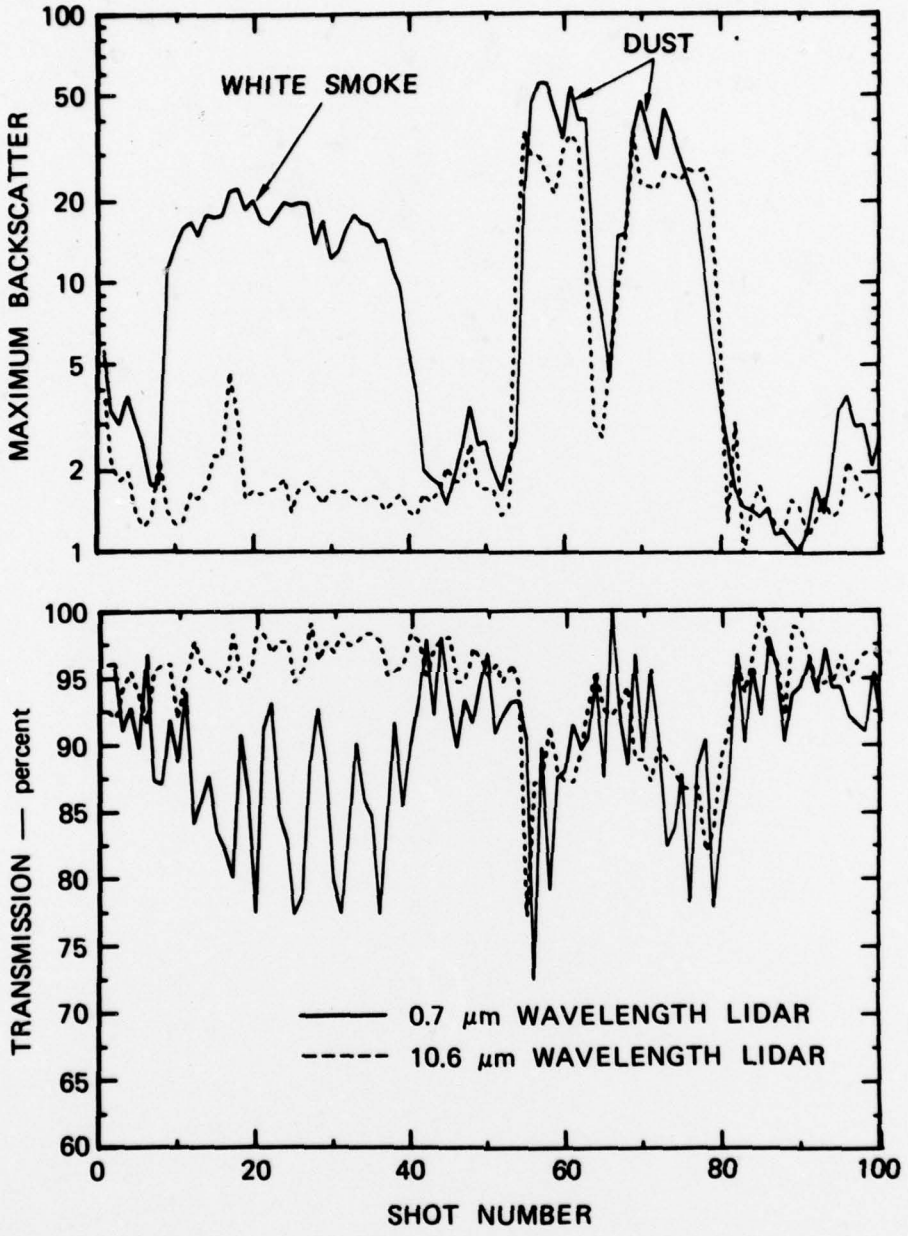

FIGURE 10 TRANSMISSION AND MAXIMUM BACKSCATTER OBSERVED BY THE TWO-WAVELENGTH LIDAR SYSTEM FOR ROAD DUST AND WHITE SMOKE

smoke, both backscatter and transmission data derived from the 10.6-μm system are near values observed during clear-air conditions, while greater backscatter and lower transmissions are measured by the 0.7-μm system than were measured for road dust.

Figure 10 presents data for road dust and white smoke collected with a higher-sensitivity CO_2 lidar system. Although large signal levels from the dust may be processed in a nonlinear fashion, the system is more capable of observing weak backscatter returns from smoke aerosols. Again, good agreement is obtained between the two systems for observation of road dust, but white smoke is not detected on the backscatter and transmission records of the long-wavelength lidar system. It is interesting that a relatively large backscatter return is observed at shot number 17, indicating that a small dust cloud was detected. The 10.6-μm-wavelength system seems to be a good indicator of the presence of dust during smoke tests.

Experimental results reported above are consistent with earlier derived theoretical data on the wavelength dependence of optical properties for aerosols consisting of different particle sizes. Figure 11 presents a plot of the extinction-to-mass concentration ratio as a function of wavelength for three size fractions of fly-ash aerosols. Observations made on size-classified

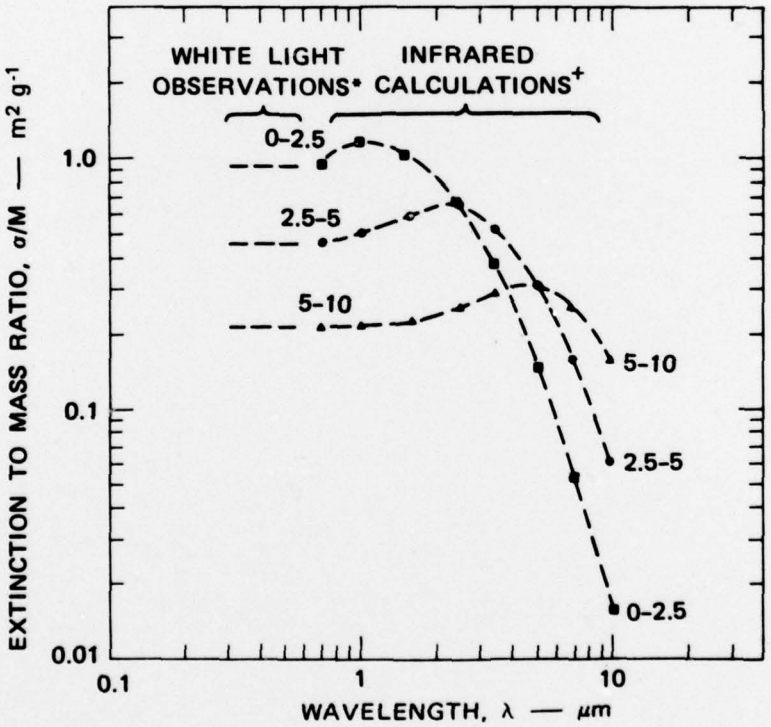

*Values measured by Uthe and Lapple for fly ash aerosols with 0-2.5, 2.5-5 and 5-10 μm diameter size fractions.

+Based on log normal size distributions fitted to measured fly ash size distributions.

FIGURE 11 DEPENDENCE OF THE EXTINCTION-TO-MASS RATIO OF FLY-ASH AEROSOLS ON PARTICLE SIZE AND WAVELENGTH OF THE LIGHT SOURCE

fly-ash fractions in the visible wavelength region agree with the theoretical data, which extends into the infrared region.[1] At short wavelengths, the extinction-to-mass ratio σ/M is larger for aerosols consisting of smaller-sized particles. However, at 10.6 μm, the value of σ/M is larger for aerosols consisting of larger-sized particles. In terms of the dust/smoke observations, the 0-to-2.5-μm-sized fraction can be equated to smoke, the 5-to-10μm fraction to road dust and the 2.5-to-5-μm fraction to background aerosols. Then, the smoke aerosols superimposed on background aerosols are easily detected at a wavelength of 0.7 μm but not at 10.6 μm. The dust aerosols are easily detected at a wavelength of 10.6 μm but not at 0.7 μm. The results of this analogy are consistent with the two-wavelength lidar observations.

The data presented in Figure 11 suggest that an optimum wavelength region exists for the remote sensing of aerosol physical density for the fly-ash aerosols. An extinction measurement in the 3-to-4-μm wavelength region can be used to evaluate mass concentration with little error resulting from uncertainties in particle size. This optimum wavelength shifts to shorter wavelengths for smaller-sized particles and to longer wavelengths for larger-sized particles. Experimental validation of a 3.39-μm laser transmissometer for monitoring mass concentration of fly-ash aerosols has recently been reported (Uthe, 1978).

C. *Results of Scheduled Smoke Tests*

Since the objective of this program was to evaluate performance of 10.6-μm wavelength lidar systems for smoke observation rather than a detailed analysis of smoke distributions and density, only intensity modulated TV displays as observed in real-time are presented for most of the data runs. Data from several runs were further processed in terms of backscatter and transmission to illustrate possible quantitative use of the two-wavelength lidar observations. These data are presented below.

The first test was conducted near 1315 MDT on 21 September 1977. The triggering level of the lidar digitizer was not correctly set at the start of the test, which caused erratic data behavior during the first few minutes of the test, as shown in Figure 12(a). (Note that the data presentations of Figure 12 were photographed from the real-time TV display and that the data could be further processed for correct display.) The wind component along the lidar/target path was variable, causing the smoke aerosols to be transported across the path near the lidar site and later near the target site. It appears that the initial smoke was not observed by the CO_2 lidar; however, at 1325 MDT, backscatter was detected that corresponds in range with backscatter from smoke observed by the ruby system. It seems that the smoke aerosols are near the detection limit of the CO_2 system and that changes in smoke density or characteristics (such as particle size) cause detection of only part of the smoke plume.

During the test conducted on 22 September, the ground conditions were relatively dry, and dust aerosols were generated by normal activity at the lidar site. The three bright areas on the TV data screen near the lidar site were caused by personnel walking between lidar vans. These "dust clouds" are more readily apparent on the 10.6-μm than the 0.7-μm wavelength lidar system. Again, the smoke aerosols are detected on only a few of the 10.6-μm lidar signatures.

---

[1]The theoretical calculations presented assumed a constant real refractive index for all wavelengths. Actual optical constants and particle sizes for smoke aerosols should be used in these calculations, and this could alter the results.

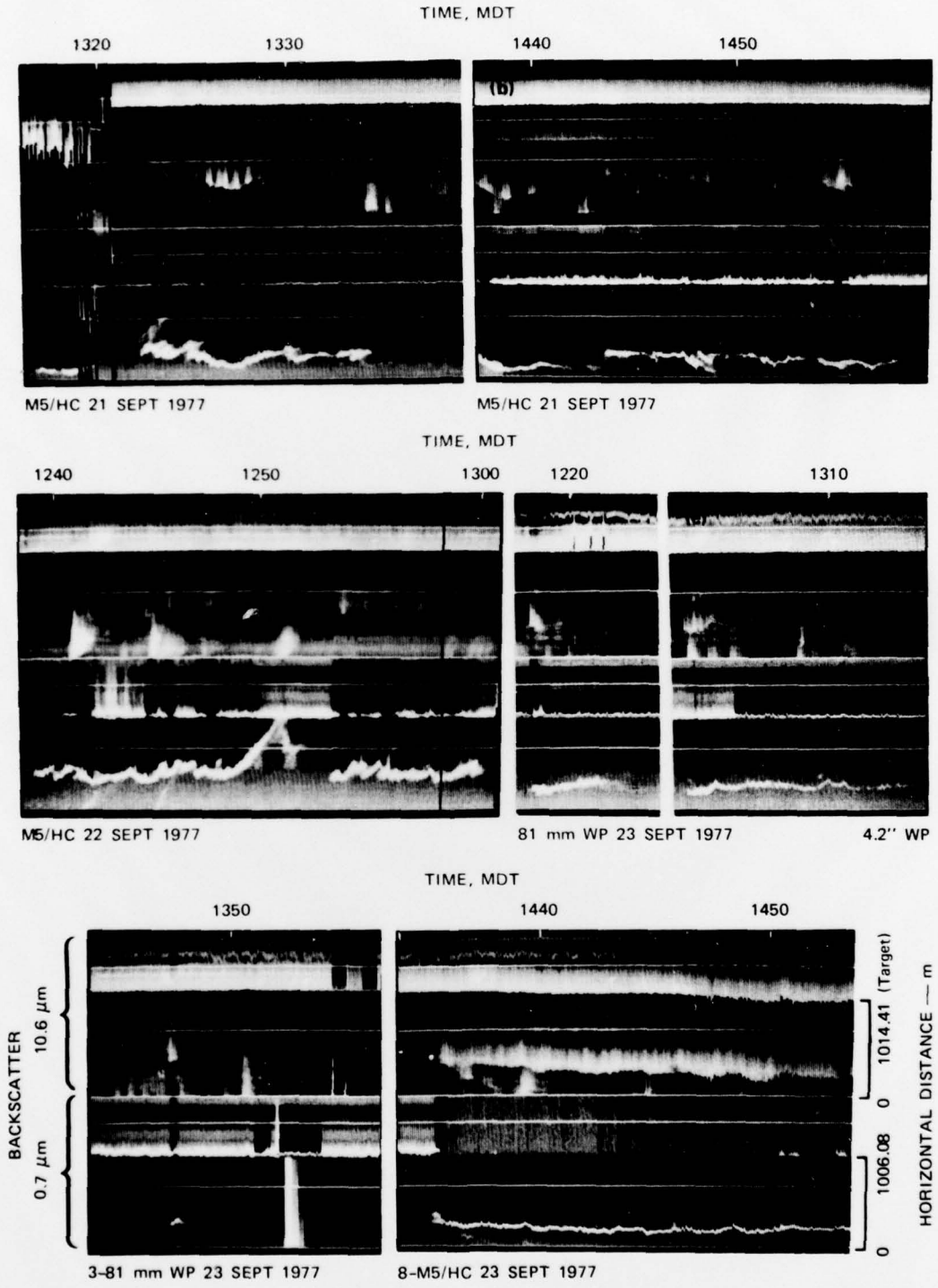

FIGURE 12 TV PRESENTATIONS OF THE TIME/DISTANCE DISTRIBUTION OF SMOKE AEROSOLS AS OBSERVED IN REAL TIME BY THE TWO-WAVELENGTH LIDAR SYSTEM

The initial smoke aerosols were detected with the CO_2 system on the first three smoke tests conducted on 23 September, but were not detected a few minutes later. The erratic data display shown after 1350 MDT is a result of the calibration run (see Section IV-A).

The final test was conducted with eight M5 smoke pots creating a relatively dense smoke plume. Smoke was regularly detected with the long-wavelength lidar. The Mark IX lidar detector gate controlling the target return was switched for maximum sensitivity to attempt to observe the target return in the presence of the dense smoke. However, as shown in Figure 12(g), the target return was observed on only a few laser firings.

For the data collected during the four smoke tests on 23 September, the digital (magnetic tape) data records were processed for maximum backscatter along the lidar/target path (normalized to 1.0 for the minimum value) and for one-way transmission over the path (normalized to 100% for the maximum target return). Figure 13 presents the results for the first smoke test conducted on this day. The smoke aerosols were observed for about four minutes after the first return observed on the visible lidar system and less than one minute on the infrared lidar system. The maximum backscatter was about four times greater on the visible data records. While the smoke was detectable on the transmission records derived from the infrared lidar (greater than 50%), the transmission for the visible record was less than 10%.

Similar results were obtained during the second smoke test (Figure 14). However, in this test the smoke was detected at longer times after the initial detection and the transmission values at the two wavelengths were in closer agreement. Figure 15 shows that the smoke aerosols generated during the third test (three rounds of 81-mm WP smoke) were detected by both lidar systems for only about a one-minute period. Again the smoke particles had greater backscatter and extinction at the 0.7-μm than the 10.6-μm wavelength. Although three rounds of smoke were detonated, as opposed to one round during the first test (Figure 13), less effect on visible laser propagation and about the same effect on infrared laser propagation was recorded.

The fourth test of the day provided the densest smoke observed during the field program. Even with the most sensitive setting of the target gate, the target return fell below the noise level of the Mark IX receiver/detector system, as shown in Figure 16. These data show that the lowest transmission that could be measured with the visible wavelength lidar was about 0.3% and that the transmission was below this value for most of the observations. Approximately 15 minutes after the initial smoke return at 1435 MDT, the smoke density decreased as shown by the infrared backscatter and visible transmission records. However, the visible backscatter does not indicate this decrease in aerosol density. This may be explained because the large returns from the smoke are beyond the detector saturation level of the Mark IX lidar system (see Section IV-A). Another peculiarity is the lower transmission recorded by the infrared lidar at the time of decreasing aerosol density. This may have been the result of the laser beam intercepting a smaller area of the passive target. The beam had been raised so that only a part of CO_2 energy pulse intercepted the target. This reduced the possibility of saturation of the lidar electronics by the large target return and also reduced ground clutter along the path (it was determined that much of the clear air return along the path was a result of reflected energy from surface features). Clearly, this initial field program revealed several instrumentation deficiencies that require attention before quantitative information on aerosol optical and physical densities may be reliably obtained by lidar systems.

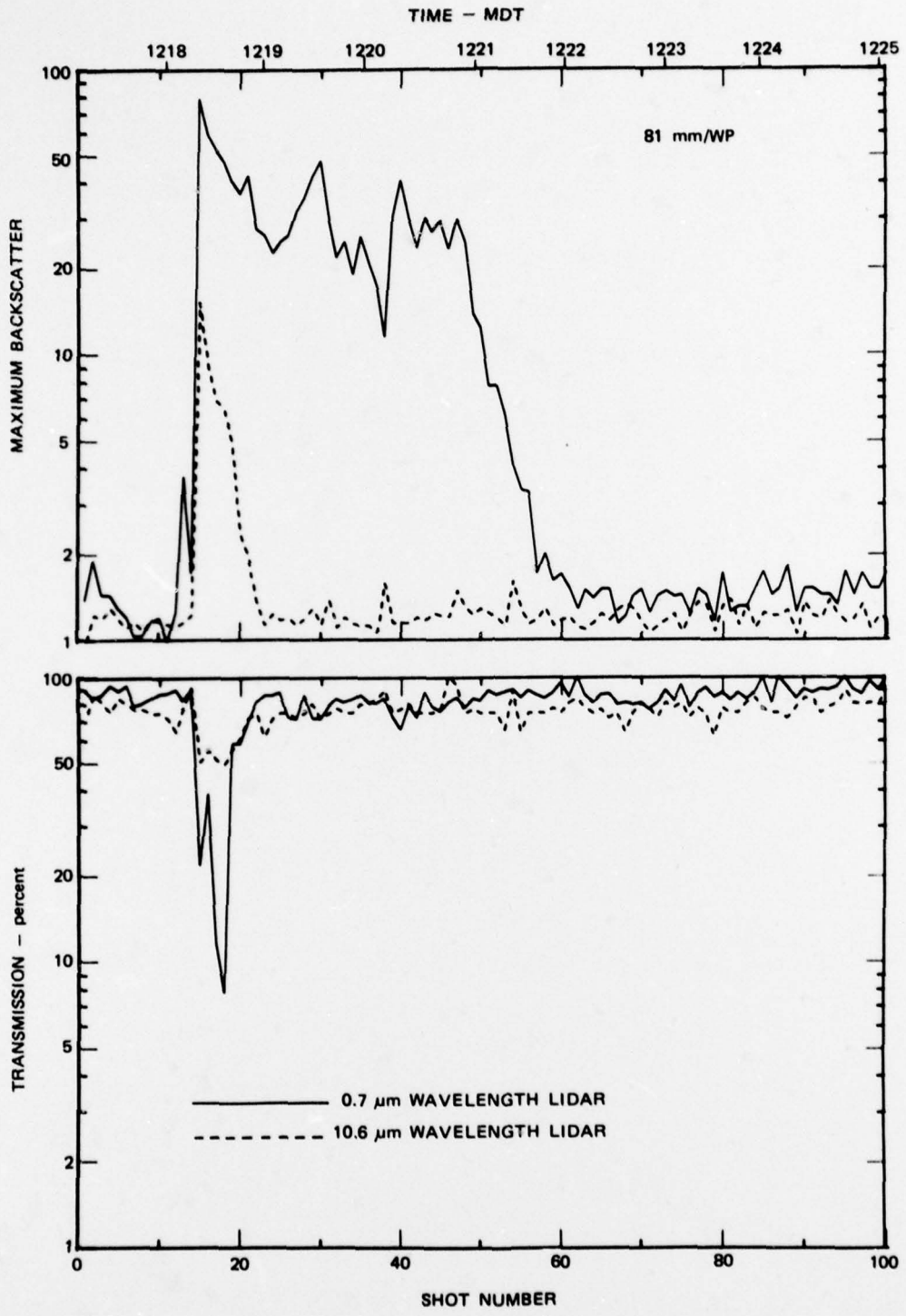

FIGURE 13 TRANSMISSION AND MAXIMUM BACKSCATTER OBSERVED BY THE TWO-WAVELENGTH LIDAR SYSTEM FOR THE FIRST TEST ON 23 SEPTEMBER 1977

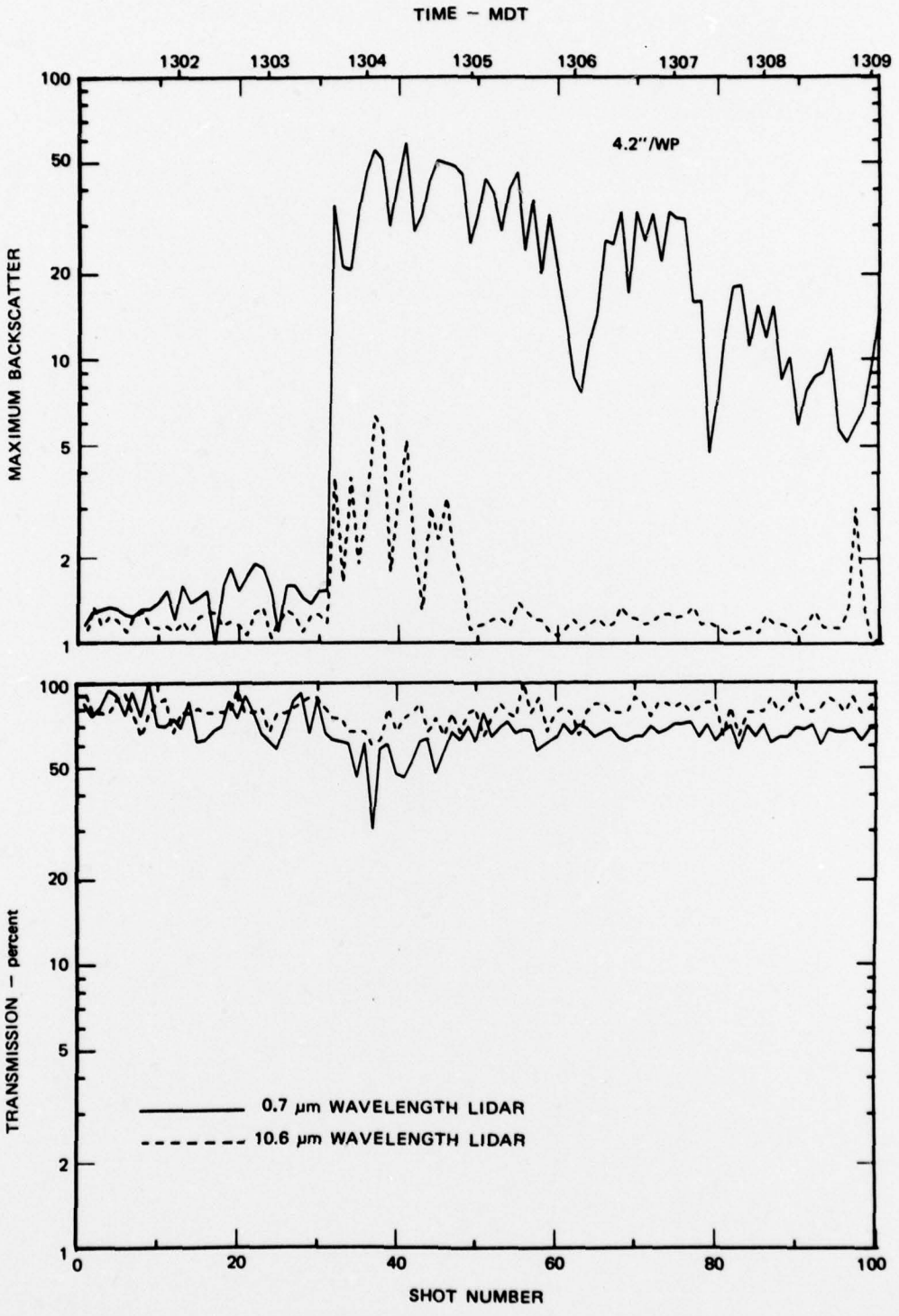

FIGURE 14 TRANSMISSION AND MAXIMUM BACKSCATTER OBSERVED BY THE TWO-WAVELENGTH LIDAR SYSTEM FOR THE SECOND TEST ON 23 SEPTEMBER 1977

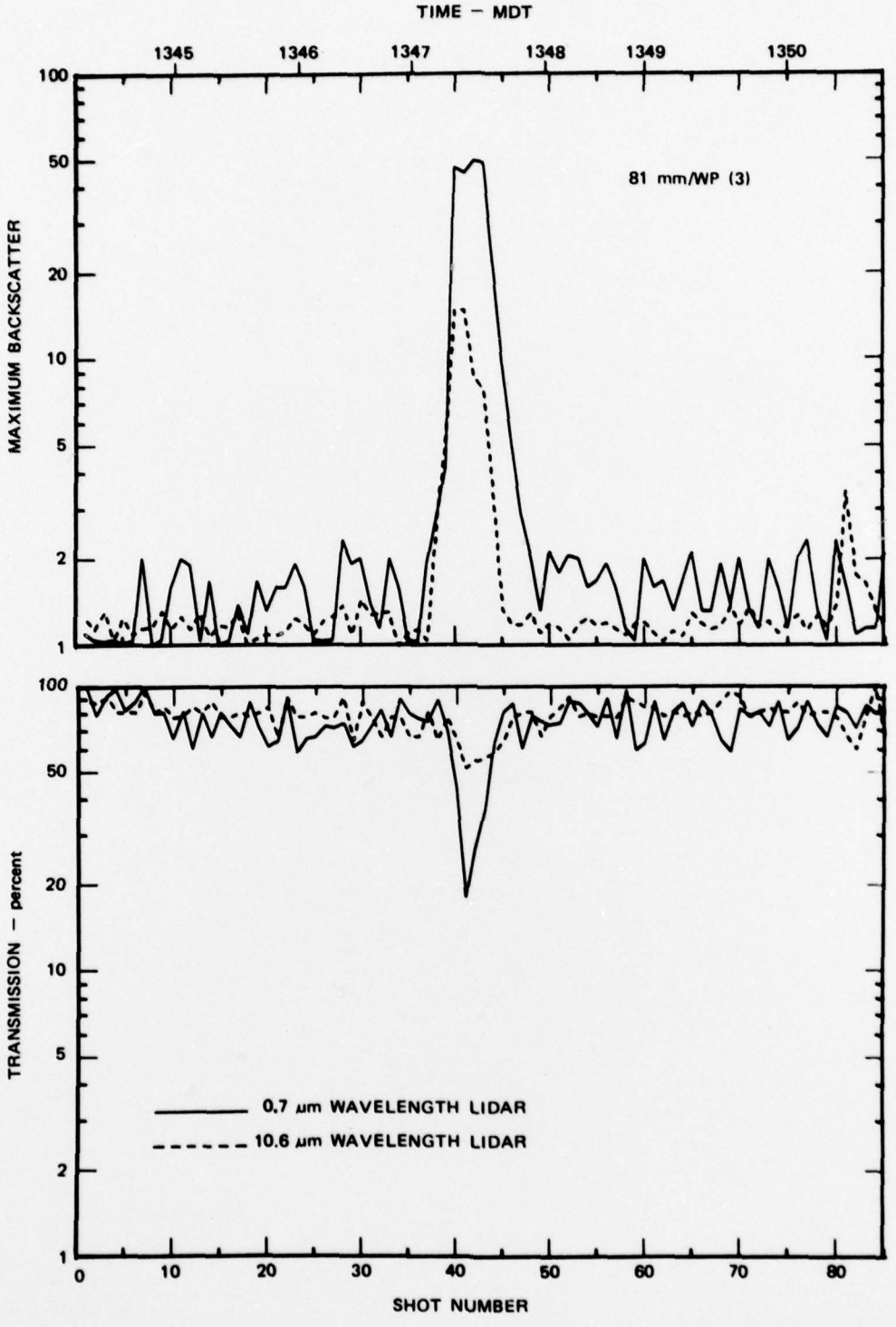

FIGURE 15 TRANSMISSION AND MAXIMUM BACKSCATTER OBSERVED BY THE TWO-WAVELENGTH LIDAR SYSTEM FOR THE THIRD TEST ON 23 SEPTEMBER 1977

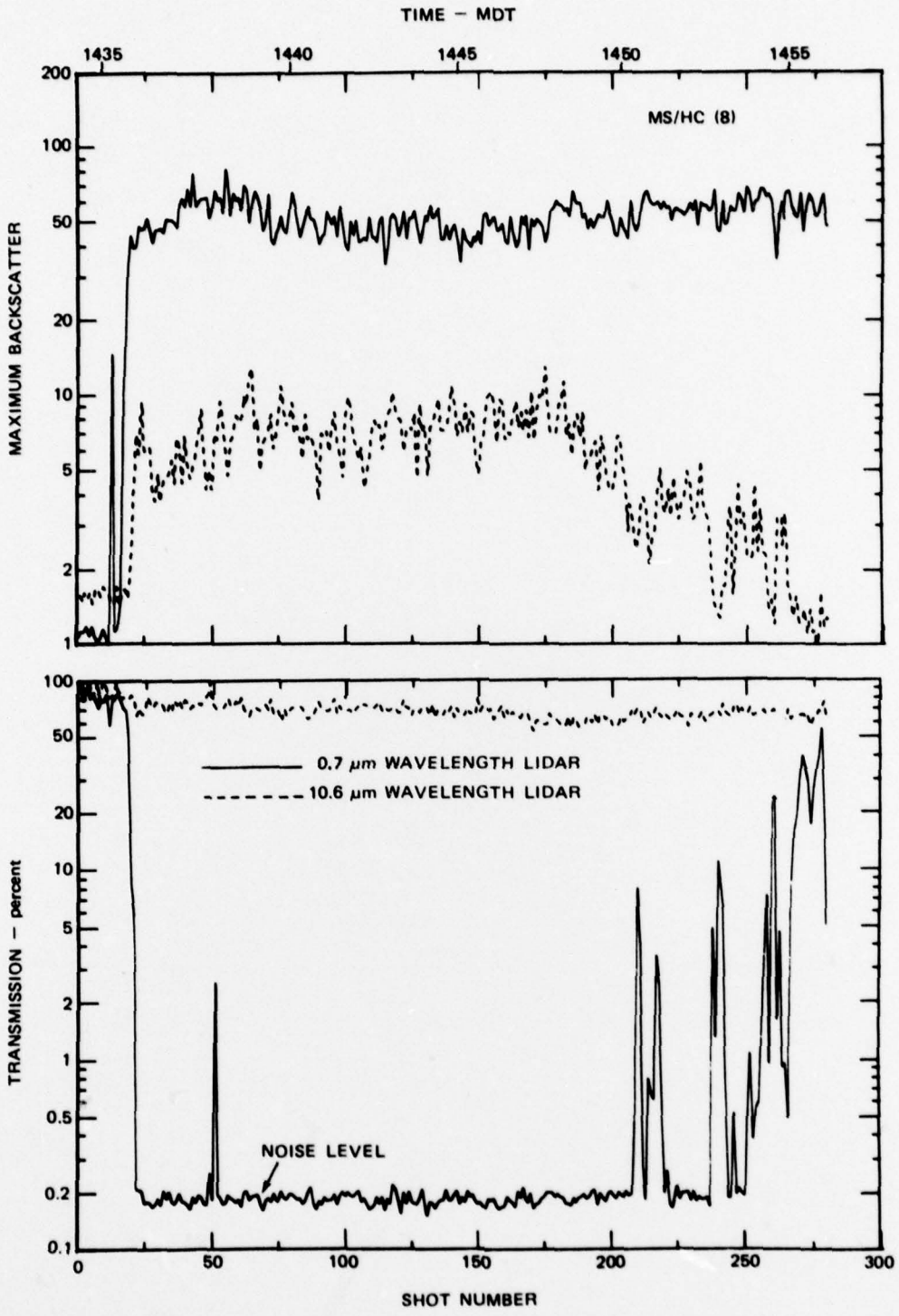

FIGURE 16 TRANSMISSION AND MAXIMUM BACKSCATTER OBSERVED BY THE TWO-WAVELENGTH LIDAR SYSTEM FOR THE FOURTH TEST ON 23 SEPTEMBER 1977

V CONCLUSIONS AND RECOMMENDATIONS

The basic objective of this study was to provide information required for procuring an optimum instrumentation system for the remote observation of dense smoke aerosols. An ideal system would provide real-time three-dimensional data on particle size, shape, and composition distributions, and on aerosol physical density and optical parameters at any wavelength over extended ranges with high space and time resolutions. The lidar technique provides more of the required information than any other technique, but present and near-future lidar systems cannot provide all the information asked of the ideal sensor. However, the capabilities of the lidar technique are continually being extended as exemplified by this study.

The following conclusions on the capabilities of visible and 10.6-μm-wavelength lidar systems for remote aerosol observation are based on the experimental data collected on this study and on the assumption that differences in the lidar observations of smoke and dust aerosols are a result of particle size effects:

(1) Visible-wavelength lidar systems can provide information on the three-dimensional structure of relatively low-density aerosols consisting of either small or large-sized particles.

(2) 10.6-μm-wavelength lidar systems can provide information on the three-dimensional structure of low-density aerosols, providing that the aerosol consists of large sized particles.

(3) Visible-wavelength lidar systems cannot penetrate high-density aerosols consisting of small-sized particles, and therefore only the structure of the near-side clear air/aerosol interface is observed.

(4) 10.6-μm-wavelength lidar systems can provide information on the three-dimensional structure of aerosols consisting of small-sized particles only for very-high-density aerosols.

(5) Target reflected laser energy observed by a lidar system can provide a measure of the atmospheric transmission for the lidar/target path. A visible-wavelength lidar can provide transmission measurements even when relatively dense aerosols are distributed along the lidar/target path ($T>0.2\%$).

(6) Transmission measurements made with visible and 10.6-μm-wavelength lidar systems are in good agreement when aerosols along the path consist of large-sized particles. However, attenuation is significantly greater at visible wavelengths when the aerosol consists of small-sized particles.

The conclusions are consistent with theoretical data relating aerosol extinction to particle size and wavelength of the energy source. The theory also indicates that an optimum wavelength region exists for making remote aerosol density measurements independent of particle size within a given range. For particles in the size range of the smoke aerosols, the optimum wavelength region is 3-to 4-μm. Moreover, since lidar systems cannot penetrate dense aerosol clouds at visible (0.7 μm) wavelengths and are insensitive to smoke aerosols at long (10.6-μm) wavelengths, it is suggested that a 3-to-4 μm-wavelength lidar may be the optimum single-wavelength system for remote observation of dense smoke aerosols. Of course, a three-wavelength system operating at visible (or near infrared), 3-to-4 μm, and 10.6 μm would provide additional information on the characteristics of the scattering particles and provide three-dimensional data on the distribution of aerosols over a wider range of aerosol densities. The theoretical data (Figure 11) indicate that three wavelengths may provide nearly all information that can be derived on the nature of the scattering particles.

The following recommendations are made for development of an optimum lidar system for remote observations of dense smoke.

(1) Lidar receivers should be improved to accurately process large-dynamic-range signals (over 6 orders of magnitude) without bandpass limitations and nonlinear effects.

(2) Lidar transmitters at infrared wavelengths should be improved to provide energy pulses with shorter lengths and narrower beams (to avoid ground reflection).

(3) A field program should be conducted that uses short-wavelength (0.7 or 1.06 μm), mid-wavelength (3-to-4 μm), and long-wavelength (10.6 μm) lidar systems to observe dense smoke aerosols, to provide data for optimization of lidar wavelength and lidar specifications at that wavelength. The data could also be used for evaluation of multiple- wavelength lidar techniques for aerosol characterization.

(4) Both hardware and software developments are required for implementing lidar angular scanning when using a multi-laser array and for high-speed processing and display of multi-wavelength lidar data.

(5) Backscatter and extinction values as a function of wavelength should be derived (either experimentally or theoretically) for smoke aerosols used in military programs.

REFERENCES

Johnson, W.B. and E.E. Uthe, 1971: Lidar study of the Keystone stack plume. *Atmos. Environ., 5,* 703-724.

Uthe, E.E., 1978: Remote sensing of aerosol properties using laser radar techniques. *Proceedings of the SPIE seminar on Optical Properties of the Atmosphere,* Washington, D.C., 30 March.

Uthe, E.E., and W.E. Wilson, 1977: Lidar observations of the density and behavior of the Labadie power plant plume. *Proceedings of the 4th Joint Conference on Sensing of Environmental Pollutants,* New Orleans, November 6-11, 1977.

Uthe, E.E., and R.J. Allen, 1975: A digital real-time lidar data recording, processing and display system. *Optical and Quantum Electronics, 7,* 121-129.